DALTON
FULL PAPER

First-known high-nuclearity silver–nickel carbonyl cluster: nanosized $[Ag_{16}Ni_{24}(CO)_{40}]^{4-}$ possessing a new 40-atom cubic T_d closed-packed metal-core geometry †

Jianming Zhang and Lawrence F. Dahl *

Department of Chemistry, University of Wisconsin-Madison, Madison, WI 53706, USA

Received 23rd July 2001, Accepted 5th November 2001
First published as an Advance Article on the web 28th February 2002

The redox reaction of silver acetate with $[Ni_6(CO)_{12}]^{2-}$ (**2**) in acetonitrile has afforded in low yields (≤10%) a close-packed silver–nickel carbonyl cluster: namely, the pseudo-T_d $[Ag_{16}Ni_{24}(CO)_{40}]^{4-}$ tetraanion (**1**) as the $[PPh_3Me]^+$ salt. This well-defined, dark brown bimetallic cluster, which is air-unstable and light-sensitive, is the first example of a microscopic ccp chunk of quasi-silver metal that is stabilized by close-packed carbonyl-ligated transition-metal layers. The overall 40-atom metal-core geometry, which corresponds to a heretofore unknown 36-atom T_d polyhedron encapsulating four interior atoms, may be described as a central ccp Ag_{16} kernel that is connected by direct Ag–Ni bonding with four tetrahedrally disposed equilateral triangular $Ni_6(CO)_{10}$ fragments. The particular close-packed condensation mode of each ν_2 Ni_6 triangular layer to one of the four tetrahedrally oriented Ag-centered hexagonal Ag_7 layers of the Ag_{16} kernel results in each of the four tetrahedrally-connected interior Ag atoms in the $Ag_{16}Ni_{24}$ core having a localized hcp environment. Of the 10 carbonyl groups per ν_2 Ni_6 equilateral triangle, three are each terminally coordinated to a corner Ni atom, six are each edge-connected to one of the two pairs of linked Ni atoms along the three Ni_3 edges, and the remaining one caps the inner triangle of the Ni_6 triangle. Both its structure and composition were unambiguously established *via* a single-crystal X-ray diffraction analysis with a SMART CCD area detector diffractometry system. The maximum metal-core diameter in **1** is *ca.* 0.98 nm (av.) along each of the four three-fold axes.

Introduction

Over the last several decades, much attention has been directed toward the use of bimetallic systems as homogeneous/heterogeneous catalysts in a wide variety of organic reactions.[1] In particular, for many economically important reactions such as hydrogenation of unsaturated hydrocarbons, dehydrogenation, and hydrogenolysis, research has focused on bimetallic alloys composed of Group 10 transition metals and Group 11 coinage metals.[1,2]

The fact that no high-nuclearity Ag–Ni carbonyl clusters as model systems for physical measurements had been previously reported provided an incentive to undertake an extensive synthetic exploratory investigation of redox reactions of an anionic nickel carbonyl cluster with a variety of monomeric silver complexes. It was hoped that large Ag–Ni carbonyl clusters could be isolated in sufficient quantities such that their physical/chemical properties could be determined as well as their crystal structures. Although a considerable number of high-nuclearity bimetallic carbonyl clusters containing Ni have been prepared, to our knowledge the only other bimetallic carbonyl clusters containing a ccp silver core are the extraordinary $[Ag_{13}Fe_8(CO)_{32}]^{n-}$ anions (n = 3, 4, 5),[3] of which salts of the trianion [3b] and tetraanion [3a] have been crystallographically characterized. The basic architecture of this reformulated $[(\mu_{12}\text{-Ag})Ag_{12}(\mu_3\text{-Fe(CO)}_4)_8]^{n-}$ series consists of a centered cuboctahedral Ag_{13} kernel that is stabilized by its eight triangular faces being capped with $Fe(CO)_4$ fragments. It was pointed out that the 3−/4−/5− charged members of this series may be envisioned to the first approximation as $Ag^+/Ag/Ag^-$ cryptate guests, respectively, occupying the $[Ag_{12}\{\mu_3\text{-Fe(CO)}_4\}_8]^{4-}$ crypt- and host.[3b] In support of this viewpoint, both EHMO [3a] and LDF [3c] calculations are in accordance with the EPR spectrum [3a] of the paramagnetic tetraanion which revealed the unpaired electron to be strongly coupled with the centered (interstitial) silver atom but still delocalized over the entire metal framework. It was proposed that the entire $(\mu_{12}\text{-Ag})Ag_{12}Fe_8$ core acts as a quantum dot in which the metal valence electrons are confined.[3d]

Teo, Zhang, and co-workers [4] have prepared and experimentally/theoretically characterized a highly renowned, unique series of vertex-sharing centered polyicosahedra consisting of bimetallic (Au–Ag) and trimetallic (Au–Ag–M; M = Ni, Pd, Pt) supraclusters (with centered M or Au atoms) which possess organophosphine/halide ligands.

The utilization of the $[Ni_6(CO)_{12}]^{2-}$ dianion (**2**) [5] as a reducing agent as well as a Ni and/or CO source in reactions with monomers or small metal clusters has given rise to a large number of extraordinary monometallic, bimetallic and trimetallic carbonyl clusters.[6–20] Particularly noteworthy is a recent exploratory investigation of redox reactions of **2** with a variety of monomeric Cu(I) and Cu(II) complexes.[20] This research led to the reaction of **2** with $CuBr_2$ that produced the first example of a close-packed Cu–Ni carbonyl cluster with a geometrically unprecedented 32-atom metal polyhedron (encapsulating three interior metal atoms) composed of three equilateral triangular 10-/15-/10-atomic layers stacked in a pseudo-D_{3h} hcp arrangement; its formulation as a $[Cu_xNi_{35-x}(CO)_{40}]^{5-}$ pentaanion (with x = 3 or 5) was based upon the low-temperature CCD X-ray crystallographic determination coupled with an elemental analysis and X-ray fluorescence measurements which are consistent with the metal core being either Cu_5Ni_{30} or Cu_3Ni_{32} (*i.e.*, because X-rays are scattered by the electrons of an

† Dedicated by L. F. D. to Professor Dr. Wolfgang Beck, a close friend, for his many remarkable accomplishments in Transition-Metal Inorganic/Organometallic Chemistry during his highly distinguished professional career at the Institute für Anorganische Chemie der Ludwig-Maximilians-Universität, München.

DOI: 10.1039/b106615n

atom, no crystallographic assignment of each of the 35 atoms as either Ni or Cu could be made *per se*).[20]

This prominent result, together with our prior success in preparing and experimentally/theoretically analyzing the initial example of a discrete gold–nickel bimetallic-bonded species, the pseudo-T_d $[Au_6Ni_{12}(CO)_{24}]^{2-}$ dianion[19] that was isolated from the redox reaction of **2** with PPh_3AuCl, motivated us to investigate the possibility that $[Ni_6(CO)_{12}]^{2-}$ (**2**) would also be an appropriate precursor for obtaining previously unknown silver–nickel carbonyl clusters. Consequently, we have carried out a synthetic exploration involving reactions of **2** with a variety of monomeric Ag(I) reagents. Herein we report the preparation and structure/bonding analysis of the remarkable $[Ag_{16}Ni_{24}(CO)_{40}]^{4-}$ tetraanion (**1**) as the $[PPh_3Me]^+$ salt.[21]

Results and discussion

Stereochemical description of $[Ag_{16}Ni_{24}(CO)_{40}]^{4-}$ (1) and geometrical/bonding comparison with related clusters

A view of its bimetallic framework is shown in Fig. 1 and its

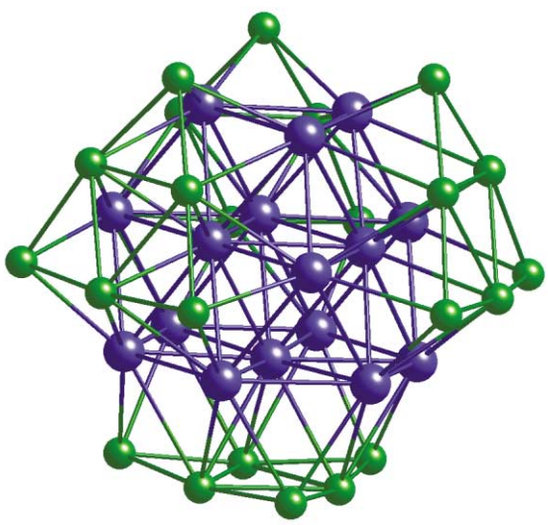

Fig. 1 $Ag_{16}Ni_{24}$ core-geometry of $[Ag_{16}Ni_{24}(CO)_{40}]^{4-}$ (**1**) of pseudo-T_d cubic symmetry: Ag (blue), Ni (green). The overall 40-atom close-packed bimetallic geometry, which corresponds to a heretofore unknown 36-atom T_d polyhedron encapsulating four interior atoms, consists of a central ccp Ag_{16} kernel composed of a three-layer [a(Ag_3) b(Ag_6) c(Ag_7)] sequence along each of the four symmetry-equivalent ⟨111⟩ cubic directions. Each Ag-centered hexagonal Ag_7 layer is directly connected by only Ag–Ni bonding interactions to four tetrahedrally disposed ν_2 Ni_6 triangles, which are oriented such that each of the four interior Ag atoms has a localized hcp environment. Under assumed T_d symmetry, the $Ag_{16}Ni_{24}$ core is comprised of four interior Ag(A), 12 surface Ag(B), 12 interior triangular Ni(A), and 12 outer triangular (corner) Ni(B) atoms.

entire geometry in Fig. 2. The entire tetraanion (**1**) possesses pseudo-T_d symmetry. Its 40-atom bimetallic core may be described as a central ccp Ag_{16} kernel which is tetrahedrally connected by direct Ag–Ni bonding to four triangular $Ni_6(CO)_{10}$ ligands. Each Ni_6 layer may be viewed as a hcp extension of the inner Ag_{16} kernel along one of the four symmetry-equivalent three-fold axes such that each of the four interior Ag atoms is encapsulated by 12 hcp metal atoms.

Each $Ni_6(CO)_{10}$ ligand may be formulated as $Ni_6(CO)_3(\mu\text{-}CO)_6(\mu_3\text{-}CO)$ in order to designate the three different kinds of coordination modes of the ten carbonyl groups to the ν_2 Ni_6 equilateral triangle. (*i.e.*, a ν_n polyhedron denotes that there are $n + 1$ equally spaced atoms along each edge). These distinct carbonyl linkages are: (1) three terminal COs, each of which is coordinated to a corner Ni atom; (2) six doubly bridging μ-COs, each of which is connected to one pair of adjacent Ni atoms

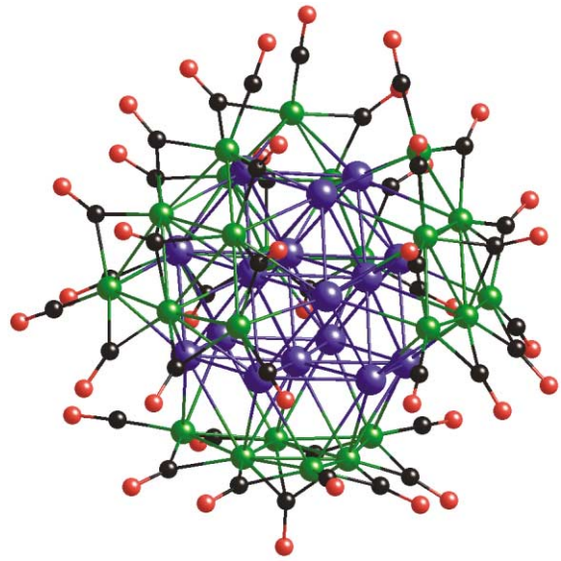

Fig. 2 Configuration of the entire $[Ag_{16}Ni_{24}(CO)_{40}]^{4-}$ tetraanion (**1**), which possesses a $Ag_{16}Ni_{24}$ core that is surrounded by a pseudo-T_d 40-carbonyl polyhedron. Each of the four $Ni_6(CO)_{10}$ fragments, which are tetrahedrally connected to the central Ag_{16} kernel, may be formulated as $Ni_6(CO)_3(\mu\text{-}CO)_6(\mu_3\text{-}CO)$ in order to designate the three terminal, six edge-bridging, and one face-capping COs coordinated to the ν_2 Ni_6 equilateral triangle.

along the three Ni_3 edges; and (3) one triply bridging μ_3-CO that caps the inner triangle of the ν_2 Ni_6 triangle.

There are no reported examples of any bimetallic cluster containing a microscopic chunk of silver metal stabilized by outer Group 10 (Ni, Pd, Pt) metal atoms. Under pseudo-T_d symmetry, the 16 ccp silver atoms in **1** can be divided into two sets consisting of four symmetry-equivalent internal Ag(A) atoms and 12 symmetry-equivalent surface Ag(B) atoms. Table 1 shows that the tetrahedral linkage of the four internal Ag(A) atoms gives rise to six Ag(A)–Ag(A) connectivities with a mean of 2.97 Å. On the other hand, the 24 Ag(A)–Ag(B) and 18 Ag(B)–Ag(B) connectivities have virtually identical means of 2.83 and 2.84 Å, respectively, that are much shorter. The overall mean of 2.85 Å for the 48 Ag–Ag distances in the ccp Ag_{16} kernel of **1** compares favorably with that of 2.89 Å in silver metal.[22] These mean Ag–Ag distances fall within the range of 2.7–3.1 Å observed for several other types of crystallographically determined bimetallic/trimetallic silver clusters possessing silver cores. These include: (1) the Teo/Zhang series of vertex-sharing polyicosahedral suprastructures containing Au-centered bimetallic (Au–Ag) and Au-/M-centered trimetallic (Au–Ag–M; M = Ni, Pd, Pt) clusters,[4] as exemplied by $[(Ph_3P)_{10}Au_{12}Ag_{12}MCl_7]^+$ as the $[SbF_6]^-$ salt for M = Ni and as the Cl^- salt for M = Pt (intrapentagonal/interpentagonal Ag–Ag means of 2.89 Å/2.94 Å for M = Ni and 2.90 Å/2.95 Å for M = Pt);[4b] (2) the previously mentioned paramagnetic $[Ag_{13}(\mu_3\text{-}Fe(CO)_4)_8]^{4-}$ tetraanion (as the $[N(PPh_3)_2]^+$ salt)[3] of pseudo-O_h symmetry which possesses a Ag-centered Ag_{13} cuboctahedral geometry with all eight triangular faces capped by trigonal bipyramidal $Fe(CO)_4$ fragments [interior–surface Ag(i)–Ag(s) mean of 2.92 Å {range, 2.882(1)–3.001(1) Å}; Ag(s)–Ag(s) mean of 2.92 Å {range, 2.826(1)–3.106(1) Å}];[3] (3) $Ag_6\{Fe(CO)_4\}_3\{\mu_3\text{-}(Ph_2P)_3CH\}$ of pseudo-C_3 symmetry whose geometry is best described as a Ag_3 triangle of vertex-shared Ag_3Fe tetrahedra [Ag–Ag mean of 2.91 Å (range, 2.817(1)–3.065(1) Å)];[23] and (4) planar raft-like heterometallic ν_2 Ag_3M_3 triangular clusters (with an inner equilateral Ag_3 triangle) which include $[Ag_3Rh_3H_9\{(MeCH_2PPh_2)_3\}_3]^{3+}$ (Ag–Ag mean, 2.98 Å),[24a] $Ag_3M_3(CO)_{12}(Me_2PCH_2CH_2PMe_2)_3$ (Ag–Ag mean, 2.84 Å for both M = Nb or Ta),[24b] and $Ag_3Co_3(CNR)_{12}$ (R = 2,6-$C_6H_3Me_2$) (Ag–Ag mean, 2.84 Å).[24c]

Table 1 Comparison of corresponding means under assumed T_d ($\bar{4}3m$) cubic symmetry for the metal–metal connectivities in $[Ag_{16}Ni_{24}(CO)_{40}]^{4-}$ (**1**)

Metal–metal connectivities[a,b]	N[c]	Mean distance/Å	Range/Å
Ag(A)–Ag(A)	6	2.97	2.939(2)–2.984(2)
Ag(B)–Ag(B)	18	2.84	2.792(2)–2.883(2)
Ag(A)–Ag(B)	24	2.83	2.790(3)–2.858(2)
Ni(A)–Ni(A)	12	2.67	2.626(3)–2.700(3)
Ni(A)–Ni(B)	24	2.42	2.416(2)–2.441(3)
Ag(A)–Ni(A)	12	2.80	2.781(3)–2.815(3)
Ag(B)–Ni(B)	24	2.69	2.661(3)–2.738(3)
Ag(B)–Ni(A)	24	2.93	2.863(3)–3.051(3)

[a] Ag(A) designates the four symmetry-equivalent interior silver atoms that are tetrahedrally coordinated to one another; Ag(B) designates the 12 symmetry-equivalent surface silver atoms. [b] Ni(A) designates the 12 symmetry-equivalent nickel atoms in the *inner* triangles and Ni(B) the 12 symmetry-equivalent nickel atoms in the *outer* triangles of the four ν_2 triangular Ni_6 ligands. [c] N denotes the number of symmetry-equivalent metal–metal connectivities in **1**.

Particularly relevant is that from SCF–X_α MO calculations of $M_2(form)_2$ [where M = Ag(I), Cu(I); form denotes *p*-Me-$C_6H_4NCHNC_6H_4$-*p*-Me], which possess short metal–metal distances [*viz.*, Ag–Ag, 2.705(1) Å; Cu–Cu, 2.497(2) Å], Cotton, *et al.*[25a] concluded "that there is little or no direct metal–metal bonding in these molecules". Recent density functional theory (DFT) calculations were also performed by Cotton *et al.*[25b] on two other Group 11 (Cu, Ni, Au) molecular compounds containing very close Cu(I)–Cu(I) contacts: namely, on the pseudo-C_{2h} $Cu_2(hpp)_2$ (where hpp^- denotes $C_7N_3H_{12}^-$), which has a short Cu(I)–Cu(I) distance of 2.453(1) Å, and on the pseudo-D_{3h} $Cu_3(RNNNNNR)_3$ (where R denotes *p*-tolyl substituents modeled as H atoms), which consists of a linear array of Cu(I) atoms bridged by each of three RN_5R^- ligands at Cu(I)–Cu(I) distances of only 2.353(2) Å. For both compounds, the results of DFT-optimized geometries closely conformed to the crystallographically determined geometries without the necessity of invoking any covalent metal–metal bonding (*i.e.*, the short Cu ··· Cu contacts were attributed to a combination of strong Cu–N bonding and very short ligand bite distances).[25b] Because the cohesive energy of silver metal, estimated by the standard enthalpy of formation of the gaseous metal atom, is only 285 kJ mol^{-1} *versus* 338 kJ mol^{-1} for copper, 369 kJ mol^{-1} for gold, and 429 kJ mol^{-1} for nickel,[26] it is apparent that the above-mentioned Ag(I)–Ag(I) distances imply at most weakly attractive dispersion forces. It follows that the stabilization of the ccp Ag_{16} quasi-metal kernel in **1** must be a consequence of the cumulative effects of a large number of *weak* delocalized Ag–Ag bonding interactions. The large variations of the Ag–Ag distances found in the above clusters are attributed to these unusually weak Ag–Ag bonding interactions which result in marked geometrical deformations that are generated from solid-state ligand–ligand steric repulsions and packing effects.

Of interest is a comparison in **1** of the means of the symmetry-equivalent Ag–Ni and Ni–Ni distances under assumed T_d symmetry (Table 1). In **1** there are two different kinds of nickel atoms—namely, Ni(A) and Ni(B) which designate the *inner* and *outer* Ni_3 triangle, respectively, in each of the four $Ni_6(CO)_{10}$ ligands. Consequently, the 60 Ag–Ni connectivities consist of three different sets: namely, 12 symmetry-equivalent Ag(A)–Ni(A), 24 symmetry-equivalent Ag(B)–Ni(A), and 24 symmetry-equivalent Ag(B)–Ni(B) connectivities with means of 2.80, 2.93, and 2.69 Å, respectively. These markedly different means suggest that the 12 surface Ag(B) atoms form much stronger bonding interactions with the outer triangular Ni(B) atoms than those between the four interior Ag(A) and the inner triangular Ni(A) atoms. The considerably longer Ag(B)–Ni(A) connectivities reflect significantly weaker bonding interactions which are ascribed to the translational deformation of each ν_2 Ni_6 triangle from a regular hcp stacking with the adjacent bonding Ag_7 layer (*vide infra*).

The approximately planar $Ni_6(CO)_3(\mu\text{-}CO)_6$ fragment of each $Ni_6(CO)_3(\mu\text{-}CO)_6(\mu_3\text{-}CO)$ ligand (*i.e.*, without the triply bridging CO) is closely related to the middle $Ni_6(CO)_3(\mu\text{-}CO)_6$ layer of the three-layer $[Ni_{12}(CO)_{21}H_{4-n}]^{n-}$ anions (n = 2, 3, 4);[27] the middle layer and two outer $Ni_3(CO)_3(\mu\text{-}CO)_3$ layers are arranged in a pseudo-D_{3h} conformation. Under T_d symmetry the intratriangular Ni–Ni connectivities within the four ligands of **1** consist of 12 noncarbonyl-(edge-bridged) Ni(A)–Ni(A) and 24 carbonyl-(edge-bridged) Ni(A)–Ni(B) distances with means of 2.67 and 2.42 Å, respectively. The 0.25 Å shorter Ni(A)–Ni(B) connectivities relative to the Ni(A)–Ni(A) ones are readily ascribed to the much stronger carbonyl-bridged Ni–Ni interactions due primarily to dominant localized three-center Ni–C(O)–Ni bonding. These markedly different means closely match the corresponding means of the middle $Ni_6(CO)_3(\mu\text{-}CO)_6$ layers in the $[Ni_{12}(CO)_{21}H_2]^{2-}$ dianion as the $[AsPh_4]^+$ salt (2.66 and 2.43 Å), the $[PPh_4]^+$ salt (2.66 and 2.43 Å), and the $[N(PPh_3)_2]^+$ salt (2.65 and 2.43 Å) and in the $[Ni_{12}(CO)_{21}H]^{3-}$ trianion as the $[AsPh_4]^+$ salt (2.68 and 2.42 Å).[27a,b] The much shorter mean of 2.42 Å for the carbonyl-bridged Ni(A)–Ni(B) interactions in **1** also compares favorably with that for the carbonyl-bridged Ni–Ni interactions of the $Ni_3(CO)_3(\mu\text{-}CO)_3$ fragments contained in the $[Ni_6(CO)_{12}]^{2-}$ dianion (2.38 Å),[5a,28] in the $[Ni_9(CO)_{18}]^{2-}$ dianion (2.39 Å),[29] and in the $[Ni_5(CO)_{12}]^{2-}$ dianion (2.36 Å).[30] The mean terminal, doubly bridging, and triply bridging C–O distances in **1** are 1.14, 1.17, and 1.19 Å, respectively. The terminal carbonyl ligands in **1** lie essentially in the mean plane of each ν_2 Ni_6 triangle, while the edge-bridging carbonyls are bent out-of-the mean Ni_6 plane in directions away from the Ag_{16} kernel.

Bonding analysis *via* electron-counting schemes and resulting implications

The observed number of metal cluster valence electrons (CVEs) in the $Ag_{16}Ni_{24}$ core of $[Ag_{16}Ni_{24}(CO)_{40}]^{4-}$ (**1**) is 500 electrons [*i.e.*, 16 × 11 (Ag) + 24 × 10 (Ni) + 40 × 2 (CO) + 4 (charge) = 500]. The predicted number of CVEs obtained by the combined application of the electron-counting Shell model and inclusion principle[31] (as illustrated by Teo and Zhang[32] for other closed-packed metal clusters with interior atoms) is 492 electrons: for a close-packed high-nuclearity metal cluster, the calculated electron count is given by $N = 2(6G_n + K)$, where G_n is the total number of close packed atoms (*viz.*, 40), and $K = 6$ for **1** (which has an internal Ag_4 tetrahedron encapsulated by 12 Ag and 24 Ni atoms). Thus, in the case of the $Ag_{16}Ni_{24}$ cluster (**1**), the total number of calculated electrons (N) is equal to $2 \times (6G_n + K) = 2 \times (6 \times 40 + 6) = 492$ electrons. The PSEP model developed by Mingos[33] for high-nuclearity close-packed metal clusters states that the total valence electron count, N, is given by $\Delta_i + 12n_s$, where Δ_i is the electron count for the central fragment (*viz.*, 60 for an interstitial Ag_4 tetrahedron) and n_s is the number of surface atoms (*viz.*, 36). Thus, the predicted electron count for **1** is also 492.

A close examination of the geometry of the $Ag_{16}Ni_{24}$ core provides a possible explanation why the observed electron count of the CVEs is eight electrons higher than the calculated

one. Each Ni_6 layer in the identical four-layer [a(Ag_3) b(Ag_6) c(Ag_7) b(Ni_6)] sequence along each symmetry-equivalent body-diagonal ⟨111⟩ cubic direction under assumed T_d symmetry was found to deviate significantly from a regular closest-packed layering. Although the three silver layers along each ⟨111⟩ direction of the Ag_{16} kernel closely adhere to ccp stacking, each ν_2 Ni_6 triangle is significantly displaced from a *regular hcp* stacking of the three localized [b(Ag_6) c(Ag_7) b(Ni_6)] layers; this translational shift perpendicular to the localized three-fold stacking axis for each of the four $Ni_6(CO)_3(\mu\text{-}CO)_6(\mu_3\text{-}CO)$ ligands results in a lowering of the overall pseudo-symmetry of the tetraanion from cubic T_d toward tetragonal D_{2d} ($\bar{4}2m$). This symmetry breakdown is attributed to the large size-difference between the Ag and Ni atoms.[34]

The formal removal of the triply bridging CO from each of the $Ni_6(CO)_3(\mu\text{-}CO)_6(\mu_3\text{-}CO)$ ligands would decrease the resulting observed electron count by eight electrons to the same calculated value of 492 obtained from both the Teo/Zhang and Mingos models. Hence, another possible explanation for the eight-electron difference between the observed and calculated electron counts is that the non-conformity of **1** to these models is a consequence of the "extra" triply bridging COs being an essential ingredient for providing the required electronic stabilization of the Ag–Ni bonding interactions.

IR spectral analysis of $[Ag_{16}Ni_{24}(CO)_{40}]^{4-}$ (1) and resulting implications

An IR spectrum of **1** in MeCN solution exhibits strong carbonyl absorption bands at 2026 cm^{-1} and 1891 cm^{-1}. The higher frequency band is assigned to terminal COs and the lower one to doubly bridging COs. It is not surprising that no lower frequency band characteristic of the four triply bridging COs is observed in that such a band would be relatively weak.

The 43 cm^{-1} upward shift of the terminal CO band in **1** relative to the corresponding one in the $[Ni_6(CO)_{12}]^{2-}$ precursor [MeCN solution IR: 1983 (s), 1810 (m), 1785 (s) cm^{-1}] reflects a significant decrease in the negative charge on the terminal COs of the four $Ni_6(CO)_3(\mu\text{-}CO)_6(\mu_3\text{-}CO)$ fragments in **1** relative to that on the corresponding terminal COs in the $[Ni_6(CO)_6(\mu\text{-}CO)_6]^{2-}$ reductant. This marked change in IR carbonyl frequency is presumed to be a consequence of the net decrease of electron density within the terminal π^* CO orbitals in each $Ni_6(CO)_3(\mu\text{-}CO)_6(\mu_3\text{-}CO)$ fragment attributed primarily to the dispersion of negative charge over the Ag_{16} kernel in the $Ag_{16}Ni_{24}$ cluster (**1**) as well as the electron-withdrawing triply bridging μ_3-CO ligand. This indicated charge-density difference is compatible with a net transfer of electron density from the $[Ni_6(CO)_{12}]^{2-}$ dianion upon its reduction of the Ag(I) atoms in the Ag(OAc) reactant to give the resulting $[Ag_{16}Ni_{24}(CO)_{40}]^{4-}$ tetraanion which has a globally delocalized valence electron-density distribution within the ccp Ag_{16} kernel.

Experimental

Methods and materials

All reactions including sample transfers and manipulations were carried out with standard Schlenk techniques on a preparative vacuum line under nitrogen atmosphere. All flasks were light-shielded by coverage with aluminium foil. The following solvents were freshly distilled under nitrogen from the indicated appropriate drying agents immediately prior to use: tetrahydrofuran (K–benzophenone); acetone ($CaSO_4$); and acetonitrile (Na_2CO_3); diethyl ether ($CaCl_2$); methanol (Mg). Furthermore, all solvents were vigorously purged with nitrogen gas for approximately ten minutes immediately prior to application. All glassware was heat-treated and cooled to room temperature immediately prior to its usage.

The $[NMe_4]^+$ salt of the $[Ni_6(CO)_{12}]^{2-}$ dianion was prepared by a modification of the general method of Longoni, Chini, and Cavalieri.[5b,c] Infrared spectra were obtained on a Mattson Polaris FT-IR or a Nicolet 740 FT-IR spectrophotometer. Solution IR spectra were obtained by use of nitrogen-purged CaF_2 cells. The reported carbonyl frequencies were observed in the 1600 to 2200 cm^{-1} window; absorption bands due to solvents, atmospheric water, and decomposition products such as $Ni(CO)_4$ are not given.

Synthesis of the $[Ag_{16}Ni_{24}(CO)_{40}]^{4-}$ tetraanion

In a typical reaction, 0.37 g (0.47 mmol) of $[NMe_4]_2[Ni_6(CO)_{12}]$ was dissolved in 10 mL of MeCN. An Ag(OAc) suspension was obtained from the addition of 0.2 g (1.2 mmol) of Ag(OAc) to 20 mL of MeCN. The Ag(OAc) suspension was gradually added by use of a cannula to the $[NMe_4]_2[Ni_6(CO)_{12}]$ solution at room temperature over a period of 30 minutes. Upon the initial addition of Ag(OAc), the solution changed color from cherry-red to yellowish-brown. After the addition of Ag(OAc) was complete, the color of the solution changed to dark brown within an hour. An excess amount of $[PPh_3Me]Br$ (*i.e.*, 2.0 g in 10 mL of MeOH) was then added to form the $[PPh_3Me]^+$ salt with the cluster anion. After the solution was stirred for *ca.* 2 hours under a gentle stream of nitrogen, the nitrogen flow was increased to remove the solvent along with $Ni(CO)_4$ as one of the decomposition products.

The resulting brown-black powder was washed with 3 × 30 mL MeOH–H_2O (1 : 1 mixture) in order to remove primarily salts of the $[PPh_3Me]^+$ and $[NMe_4]^+$ counterions, as well as oxidized Ni(II) salts. The solid was then sequentially washed with a series of solvents of increasing polarity. Extraction with either pentane or diethyl ether gave a colorless solution that was discarded. The THF extraction gave a red product, which from an IR spectrum was identified as mainly the $[Ni_6(CO)_{12}]^{2-}$ dianion.

After thorough extractions with THF, the remaining brown-black powder was extracted with acetone, which resulted in a moderately concentrated dark brown solution. An IR spectrum revealed carbonyl absorption bands at 2028(ms), 1990(ms), and 1888(s, broad) cm^{-1} indicative of a mixture of at least two metal carbonyl clusters (*vide infra*). Extraction with acetonitrile gave a more concentrated solution but with the same IR bands. The acetone extraction solution was transferred to a thin (diameter, 0.5 cm), long crystallization tube under nitrogen. Diethyl ether was very slowly layered on top of the extracted solution *via* a needle syringe under nitrogen. Approximately twice the amount of diethyl ether was layered. After two weeks, shiny black crystals were observed at the interface of the two solvents. A complete X-ray crystallographic determination performed on one crystal (*vide infra*) revealed the $[Ag_{16}Ni_{24}(CO)_{40}]^{4-}$ tetraanion (**1**) as the $[PPh_3Me]^+$ salt. Yields of **1** were estimated to be ≤10% (based on Ag(OAc). The observed two IR carbonyl frequencies (*vide supra*) approximately coincide with one of the two terminal frequencies and the bridging carbonyl frequency. As yet, the identity of the other prejudged one metal carbonyl component responsible for the lower terminal carbonyl frequency (and presumably a bridging carbonyl frequency similar to that found for **1**) has not been determined. Some black solid (primarily decomposed metal) remained after the extractions. Reaction vessels were covered with aluminium foil to protect desired Ag–Ni clusters from decompositions.

Experimental efforts under different boundary conditions were carried out in attempts to optimize the yield of **1**.These included the following variations: (1) It was found that the rate of addition of Ag(OAc) to the acetonitrile solution of $[NMe_4]_2[Ni_6(CO)_{12}]$ is extremely important. Fast addition of Ag(OAc) produced a precipitated by-product. Likewise, addition of the solution of $[NMe_4]_2[Ni_6(CO)_{12}]$ to the Ag(OAc) suspension afforded an analogous precipitate. Presumably excessive redox reactions between the Ni and Ag reactants resulted in the formation of metal. Direct addition of

acetonitrile to a solid mixture of the Ni and Ag reagents also did not work; the resulting reaction was so violent that a silver mirror was formed on the flask. (2) In order to achieve a maximum separation from the different solvent extractions, multiple extractions with the same solvent were performed until the extracted solvent became colorless. On the other hand, the time element in the reaction and products-treatment is important. It was observed that **1** is markedly unstable in air, especially in solution. (3) Similar reactions of the $[Ni_6(CO)_{12}]^{2-}$ dianion were carried out in acetonitrile solution with other monomeric silver salts: namely, AgCl, AgI, and $AgNO_3$. Analogous reactions with these salts were also performed with DMSO and DMF. However, these efforts were unsuccessful. In most cases it was observed that precipitation occurred to give metal. We presume that these latter redox reactions primarily produced silver metal, because of different kinetic factors due to dissimilar solubility characteristics of these other silver reactants relative to that of silver acetate.

Characterization of $[Ag_{16}Ni_{24}(CO)_{40}]^{4-}$ (1)

This tetraanion is dark brown or black in powder form but medium brown in solution. As a powder it is insoluble in THF or any other lower-polarity organic solvent but soluble in acetone and acetonitrile; however, the powdered residue obtained from crystallization tubes did not redissolve in either solvent. The powdered compound decomposed gradually under vacuum, and much more rapidly when exposed to air, light, or water. Caution should be used when undertaking the separation of the product, because spontaneous combustion of the filter paper permeated with this compound (or the resulting decomposition products thereof) occurred upon exposure to air. Attempted measurements of the melting or decomposition point of this compound showed that there is no readily discernible difference between the powdered form of this compound and the decomposition product.

An IR spectrum (acetonitrile) of this cluster exhibited a strong maximum at 2026 cm^{-1} corresponding to terminal carbonyls and a strong maximum at 1891 cm^{-1} corresponding to the doubly bridging carbonyls.

Elemental analysis by DESERT ANALYSIS (Tucson, AZ) of the dark brown powder presumed to be **1** (as indicated from an IR spectrum) gave inconclusive results. However, the Ag/Ni mole ratio of 15.67/24.00 is consistent with that of 16/24 obtained from the CCD X-ray diffraction analysis. It is apparent that sufficient crystals of **1** need to be acquired in order to confirm the definitive composition established from the crystallographic analysis.[21]

X-Ray crystallographic determination

A black prism-shaped crystal of dimensions 0.15 × 0.10 × 0.10 mm was selected for structural analysis. Intensity data for this compound were collected with a SMART CCD area detector mounted on a Bruker P4 diffractometer equipped with graphite-monochromated Mo-Kα radiation ($\lambda = 0.71073$ Å).

$[PPh_3Me]_4[Ag_{16}Ni_{24}(CO)_{40}]\cdot 3Me_2CO\cdot 0.5C_4H_8O$, $M = 5574.4$, monoclinic, $P2_1/n$, $a = 20.0344(6)$ Å, $b = 26.3787(6)$ Å, $c = 30.2923(8)$ Å, $\alpha = 90°$, $\beta = 92.933(2)°$, $\gamma = 90°$, $V = 15987.9(7)$ Å^3, $Z = 4$, $D_c = 2.316$ Mg m^{-3}. 61215 data were obtained at 153(2) K *via* 0.3° ω oscillation frames (70 s frame^{-1}) over $4.7 \leq 2\theta \leq 50.0°$. An absorption correction (SADABS)[35] was applied [μ(Mo-Kα) = 4.764 mm^{-1}; max./min. transmission, 0.704/0.565]. The crystal structure was solved by direct methods and refined by full-matrix least squares on F^2 with SHELXTL.[36] Non-hydrogen atoms were refined anisotropically; ideal positions of hydrogen atoms were initially determined geometrically and then refined by a riding model. Refinement (2078 parameters; 2265 restraints) on 27631 independent merged data (R_{int} = 0.0994) converged at wR_2 (F^2) = 0.215 for all data with $w = 1/[\sigma^2(F^2) + (0.1030P)^2]$, where $P = [F_o^2 + 2F_c^2]/3$; $R_1(F) = 0.086$ for 13922 observed data [$F > 4\sigma(F)$]; max./min. residual electron density, 1.829/−1.833 e Å^{-3}. One of the four independent $[PPh_3Me]^+$ cations was disordered and modeled in two orientations with occupancies of 0.517(11) and 0.483(11).

CCDC reference number 180330.

See http://www.rsc.org/suppdata/dt/b1/b106615n/ for crystallographic data in CIF or other electronic format.

Acknowledgements

This research was supported by the National Science Foundation (Grants CHE-9310428 and CHE-9729555). Departmental purchase of the CCD area detector system in 1995 was made possible by the funds from NSF (Grant 9310428) and the UW-Madison Graduate School and Chemistry Department. We are most grateful to Dr Douglas R. Powell for his crystallographic help. Color figures were made with Crystal Maker, Interactive Crystallography for MacOS (David Palmer).

References and notes

1 Selected articles with references are: (*a*) J. H. Sinfelt, *Bimetallic Catalysts: Discoveries, Concepts, and Applications*, Wiley, New York, 1983; (*b*) V. Ponec, *Adv. Catal.*, 1983, **32**, 149; (*c*) W. M. H. Sachtler and R. A. van Santen, *Adv. Catal.*, 1977, **26**, 69; (*d*) J. H. Sinfelt, *Acc. Chem. Res.*, 1987, **20**, 134; (*e*) W. M. H. Sachtler and A. Yu. Stakheev, *Catal. Today*, 1993, **12**, 283; (*f*) B. C. Gates, *Catalytic Chemistry*, J. Wiley, New York, 1992; (*g*) P. Braunstein and J. Rose, in *Comprehensive Organometallic Chemistry II*, E. W. Abel, F. G. A. Stone and G. Wilkinson, eds., Elsevier, Tarrytown, NY, 1995, vol. 10, R. D. Adams, ed., ch. 7, p. 351; (*h*) G. Süss-Fink and G. Meister, *Adv. Organomet. Chem.*, 1993, **35**, 41; (*i*) N. Toshima and T. Yonezawa, *New J. Chem.*, 1998, **22**, 1179; (*j*) *Catalysis by Di- and Polynuclear Metal Cluster Complexes*, R. D. Adams and F. A. Cotton, eds., Wiley-VCH, New York, 1998; (*k*) *Metal Clusters in Chemistry*, P. Braunstein, L. A. Oro and P. R. Raithby, eds., Wiley-VCH, New York, 1999, p. 2; (*l*) *Handbook of Heterogeneous Catalysis*, G. Ertl, H. Knözinger and J. Weitkamp, eds., Wiley-VCH, New York, 1994; (*m*) *Applied Homogeneous Catalysis with Organometallic Compounds*, B. Cornils and W. A. Herrmann, eds., VCH, New York, 1996, vol. 1 (Applications), vol. 2 (Developments); (*n*) M. Ishikawa, *Adv. Catal.*, 1992, **38**, 283.

2 (*a*) I. D. Salter, *Adv. Organomet. Chem.*, 1989, **29**, 249; (*b*) I. D. Salter, in *Comprehensive Organometallic Chemistry II*, E. W. Abel, F. G. A. Stone and G. Wilkinson, eds., Elsevier, Tarrytown, NY, 1995, vol. 10, R. D. Adams, ed. ch. 5, p. 255; (*c*) I. D. Salter, in *Metal Clusters in Chemistry*, P. Braunstein, L. A. Oro and P. R. Raithby, eds., Wiley-VCH, New York, 1999, vol. 1, p. 509.

3 (*a*) V. G. Albano, L. Grossi, G. Longoni, M. Monari, S. Mulley and A. Sironi, *J. Am. Chem. Soc.*, 1992, **114**, 5708 and references therein; (*b*) V. G. Celbano, F. Calderoni, M. C. Iapalucci, G. Longoni, M. Monari and P. Zanello, *J. Cluster Sci.*, 1995, **6**, 107 and references therein; (*c*) K. Albert, K. M. Neyman, G. Pacchioni and N. Rösch, *Inorg. Chem.*, 1996, **35**, 7370; (*d*) J. Sinzig, L. L. de Jongh, A. Ceriotti, R. della Pergola, G. Longoni, M. Stener, K. Albert and N. Rösch, *Phys. Rev. Lett.*, 1998, **81**, 3211.

4 (*a*) B. K. Teo, H. Zhang and X. Shi, *J. Am. Chem. Soc.*, 1990, **112**, 8552; (*b*) B. K. Teo, H. Zhang and X. Shi, *Inorg. Chem.*, 1994, **33**, 4086; (*c*) B. K. Teo and H. Zhang, *Proc. Natl. Acad. Sci. U.S.A.*, 1991, **88**, 5067; and references therein; (*d*) B. K. Teo and H. Zhang, *Coord. Chem. Rev.*, 1995, **143**, 611; (*e*) H. Zhang and B. K. Teo, *Inorg. Chim. Acta*, 1997, **265**, 213; (*f*) B. K. Teo, A. Strizhev, R. Elber and H. Zhang, *Inorg. Chem.*, 1998, **37**, 2482; (*g*) B. K. Teo, H. Dang, C. F. Campana and H. Zhang, *Polyhedron*, 1998, **17**, 617; (*h*) B. K. Teo and H. Zhang, *J. Cluster Sci.*, 2001, **12**, 349.

5 (*a*) J. C. Calabrese, L. F. Dahl, A. Cavalieri, P. Chini, G. Longoni and S. Martinengo, *J. Am. Chem. Soc.*, 1974, **96**, 2616; (*b*) G. Longoni, P. Chini and A. Cavalieri, *Inorg. Chem.*, 1976, **15**, 3025; (*c*) A. Ceriotti, G. Longoni and G. Piva, *Inorg. Synth.*, 1989, **26**, 312.

6 (*a*) J. K. Ruff, Jr. R. P. White and L. F. Dahl, *J. Am. Chem. Soc.*, 1971, **93**, 2159; (*b*) T. Hall and J. K. Ruff, *Inorg. Chem.*, 1981, **20**, 4444.

7 A. Ceriotti, R. Della Pergola, G. Longoni, M. Manassero, N. Masciocchi and M. Sansoni, *J. Organomet. Chem.*, 1987, **330**, 237.

8 A. Ceriotti, R. Della Pergola, L. Garlaschelli, G. Longoni, M. Manassero, N. Masciocchi, M. Sansoni and P. Zanello, *Gazz. Chim. Ital.*, 1992, **122**, 365.

9 A. Ceriotti, R. Della Pergola, G. Longoni, M. Manassero and M. Sansoni, *J. Chem. Soc., Dalton Trans.*, 1984, 1181.
10 D. A. Nagaki, J. V. Badding, A. M. Stacy and L. F. Dahl, *J. Am. Chem. Soc.*, 1986, **108**, 3825.
11 A. Fumagalli, G. Longoni, P. Chini, A. Albinati and S. Brueckner, *J. Organomet. Chem.*, 1980, **202**, 329.
12 A. Ceriotti, F. Demartin, G. Longoni, M. Manassero, G. Piva, G. Piro, M. Sansoni and B. T. Heaton, *J. Organomet. Chem.*, 1986, **301**, C5.
13 (*a*) A. Ceriotti, F. Demartin, G. Longoni, M. Manassero, M. Marchionna, G. Piva and M. Sansoni, *Angew. Chem., Int. Ed. Engl.*, 1985, **24**, 696; (*b*) F. F. de Biani, C. Femoni, M. C. Iapalucci, G. Longoni, P. Zanello and A. Ceriotti, *Inorg. Chem.*, 1999, **38**, 3721.
14 (*a*) F. Demartin, C. Femoni, M. C. Iapalucci, G. Longoni and P. Macchi, *Angew. Chem., Int. Ed.*, 1999, **38**, 531; (*b*) F. Demartin, F. F. de Biani, C. Femoni, M. C. Iapalucci, G. Longoni, P. Macchi and P. Zanello, *J. Cluster Sci.*, 2001, **12**, 61.
15 (*a*) M. Kawano, J. W. Bacon, C. F. Campana and L. F. Dahl, *J. Am. Chem. Soc.*, 1996, 7869; (*b*) M. Kawano, J. W. Bacon, C. F. Campana, B. E. Winger, J. D. Dudek, S. A. Sirchio, S. L. Scruggs, U. Geiser and L. F. Dahl, *Inorg. Chem.*, 2001, **40**, 2554.
16 N. T. Tran, M. Kawano, D. R. Powell and L. F. Dahl, *J. Chem. Soc., Dalton Trans.*, 2000, 4138.
17 C. Femoni, M. C. Iapalucci, G. Longoni, P. H. Svensson and J. Woloska, *Angew. Chem., Int. Ed.*, 2000, **39**, 1635.
18 N. T. Tran, M. Kawano, R. K. Hayashi, D. R. Powell, C. F. Campana and L. F. Dahl, *J. Am. Chem. Soc.*, 1999, **121**, 5945.
19 (*a*) A. J. Whoolery and L. F. Dahl, *J. Am. Chem. Soc.*, 1991, **113**, 6683; (*b*) A. J. Whoolery Johnson, B. Spencer and L. F. Dahl, *Inorg. Chim. Acta*, 1994, **227**, 269.
20 P. D. Mlynek, M. Kawano, M. A. Kozee and L. F. Dahl, *J. Cluster Sci.*, 2001, **12**, 321.
21 Both the stoichiometry and geometry of **1** have subsequently been substantiated from a CCD X-ray diffraction analysis of the corresponding isostructural gold–nickel analogue, $[Au_{16}Ni_{24}(CO)_{40}]^{4-}$ (as the $[NMe_3Ph]^+$ salt), which was obtained from the redox reaction of gold trichloride with $[Ni_6(CO)_{12}]^{2-}$ in dimethylsulfoxide (M. A. Kozee L. F. Dahl, unpublished research). Details of its synthesis, characterization, and chemical reactivity will be presented elsewhere.
22 J. Donohue, *The Structures of the Elements*, J. Wiley & Sons, NY, 1974, pp. 209–213, 222–224.
23 C. E. Briant, R. G. Smith and D. M. P. Mingos, *J. Chem. Soc., Chem. Commun.*, 1984, 586.
24 (*a*) F. Bachechi, J. Ott and L. M. Venanzi, *J. Am. Chem. Soc.*, 1985, **107**, 1760; (*b*) F. Calderazzo, G. Pampaloni, U. Englert and J. Strähle, *J. Organomet. Chem.*, 1990, **383**, 45; (*c*) P. A. Leach, S. J. Geib and N. J. Cooper, *Organometallics*, 1992, **11**, 4367.
25 (*a*) F. A. Cotton, X. Feng, M. Matusz and R. Poli, *J. Am. Chem. Soc.*, 1988, **110**, 7077; (*b*) F. A. Cotton, X. Feng and D. J. Timmons, *Inorg. Chem.*, 1998, **37**, 4066.
26 (*a*) H. A. Skinner and J. A. Connor, *Pure Appl. Chem.*, 1985, **57**, 79; (*b*) J. A. Connor, *Top. Curr. Chem.*, 1977, **71**, 71.
27 (*a*) $[Ni_{12}(CO)_{21}H_{4-n}]^{n-}$ (n = 2, 3): R. W. Broach, Ph.D. Thesis, University of Wisconsin-Madison, 1977; (*b*) $[Ni_{12}(CO)_{21}H_{4-n}]^{n-}$ (n = 2, 3): R. W. Broach, L. F. Dahl, G. Longoni, P. Chini, A. J. Schultz and J. M. Williams, *Adv. Chem. Ser.*, 1978, **167**, 93; (*c*) $[Ni_{12}(CO)_{21}]^{4-}$ P. Chini, G. Longoni, M. Manassero and M. Sansoni, *Abstracts of the Eighth Meeting of the Italian Association of Crystallography*, Ferrara, 1977, Communication 34; (*d*) $[Ni_{12}(CO)_{21}H_{4-n}]^{n-}$ (n = 2, 3, 4): A. Ceriotti, P. Chini, R. D. Pergola and G. Longoni, *Inorg. Chem.*, 1983, **22**, 1595.
28 Recent results from liquid X-ray scattering show that the structures of both $[Ni_6(CO)_{12}]^{2-}$ and $[Pt_6(CO)_{12}]^{2-}$ adopt an overall staggered ditriangular geometry of D_3 symmetry in solution (L. Bengtsson-Kloo, C. M. Impalucci, G. Longoni and S. Ulvenlund, *Inorg. Chem.*, 1998, **37**, 4335).
29 D. A. Nagaki, L. D. Lower, G Longoni, P. Chini and L. F. Dahl, *Organometallics*, 1986, **5**, 1784.
30 G. Longoni, P. Chini, L. D. Lower and L. F. Dahl, *J. Am. Chem. Soc.*, 1975, **97**, 5034.
31 (*a*) B. K. Teo and N. J. A. Sloane, *Inorg. Chem.*, 1985, **24**, 4545; (*b*) N. J. A. Sloane and B. K. Teo, *J. Chem. Phys.*, 1985, **83**, 6520; (*c*) B. K. Teo and N. J. A. Sloane, *Inorg. Chem.*, 1986, **25**, 2315.
32 B. K. Teo and H. Zhang, *Polyhedron*, 1990, **9**, 1985 and references therein.
33 D. M. P. Mingos, *J. Chem. Soc., Chem. Commun.*, 1985, 1352; D. M. P. Mingo and L. Zhenyang, *J. Chem. Soc., Dalton Trans.*, 1988, 1657.
34 Metallic radii for 12-coordination are 1.44 Å for Ag and 1.24 Å for Ni (N. N. Greenwood and A. Earnshaw, *Chemistry of the Elements*, Butterworth-Heineman, Second Edition, 1997, pp. 1148 and 1176).
35 G. M. Sheldrick, SADABS, Program for Empirical Absorption Correction of Area Detector Data, University of Göttingen, Germany, 1996.
36 (*a*) G. M. Sheldrick, SHELXTL, Version 5, 1994; (*b*) *International Tables for Crystallography*, vol. C, A. J. C. Wilson, ed., Kluwer, Boston, MA, 1995, Tables 4.2.4.2, 4.2.6.8 and 6.1.1.4.